IEEE Open Journal of
Industry Applications

Received 15 July 2023; revised 18 September 2023; accepted 3 October 2023. Date of publication 10 October 2023;
date of current version 20 October 2023. The review of this article was arranged by Associate Editor M. Di Nardo.

Digital Object Identifier 10.1109/OJIA.2023.3323343

Investigation of Resonance Avoidance Method for Vacuum Cleaner

WOONG HWANG [1], JIMIN KIM [1], JIHOON HAN [2], WONSOO KANG [1], AND SUNGHYUK PARK [1]

[1]Energy Technology Lab, Digital Appliances, Samsung Electronics, Suwon 16677, South Korea
[2]Digital Appliances, Samsung Electronics, Suwon 16677, South Korea

CORRESPONDING AUTHOR: WOONG HWANG (Email: woong.hwang@samsung.com)

ABSTRACT Electromagnetic resonance in electric motors arises when the electromagnetic force frequency coincides with any of the motor's natural frequencies, causing excessive vibration and noise. To address this issue, it is crucial to design motors such that their natural frequencies do not closely align with the electromagnetic force frequency. However, vacuum cleaner motors operate across a broad range of speeds, generating a multitude of electromagnetic force frequencies, which makes it challenging to establish natural frequencies that can avoid all possible electromagnetic resonances. This article presents a novel approach for shifting natural frequencies by adjusting the stiffness of stator cores. By integrating an auxiliary component with various design factors into the motor, a range of natural frequencies can be achieved. An optimal natural frequency that mitigates electromagnetic resonance was identified among these modified frequencies, and the subsequent enhancement in acoustic characteristics was demonstrated.

INDEX TERMS Electromagnetic force, natural frequency, noise, resonance, stator core.

I. INTRODUCTION

Vacuum cleaners are devices that remove dust through suction generated by their motors. Recently vacuum cleaners have transitioned from canister models with power cables, which users need to drag around during cleaning, to cordless stick-type cleaners with batteries that allow for easy one-handed operation. Due to the limited battery capacity of cordless stick vacuum cleaners, users need to adjust the suction power to maximize the usage time. Consequently, cordless stick vacuum cleaners are designed with various operating modes to accommodate different levels of suction power. For example, a typical cordless stick vacuum cleaner has three operating modes: strong mode with the highest suction power, medium mode with moderate power, and weak mode with the lowest power.

Driving characteristics of various types of motors for vacuum cleaners have been extensively studied [1], [2], [3]. Among these characteristics, noise and vibration generated by motor operation significantly influence consumer preferences. There are various sources of noise and vibration in the vacuum cleaner motors. First, motors for cordless stick vacuum cleaners have a wide driving range with various operating modes, leading to the generation of different types of noise. Second, rotor unbalances generate mechanical noise. Third, electromagnetic forces produce electromagnetic noise in the motor. Finally, the rotation of the impeller creates airflow-induced noise [4], [5], [6], [7], [8], [9]. This article focuses on resonance noise generated by electromagnetic forces.

Electromagnetic force is generated due to change in magnetic flux density between a stator and a rotor of a motor during operation, which in turn causes motor vibrations [10], [11], [12], [13]. When any natural frequencies of a motor coincide its electromagnetic force frequencies, resonance occurs, leading to the generation of abnormal noise [14], [15]. There are two primary design approaches to avoid this resonance. The first method involves reducing the magnitude of the electromagnetic forces generated by the motor [16], [17], [18]. The second method focuses on modifying the stiffness of the motor's stator to ensure that its natural frequencies do not coincide with its electromagnetic forces. [19], [20]. This article investigates the latter method in detail.

Since cordless stick vacuum cleaners operate in various modes, their motors experience a range of electromagnetic forces. Recently, the number of operating modes for cordless stick vacuum cleaners has increased, and a single motor may

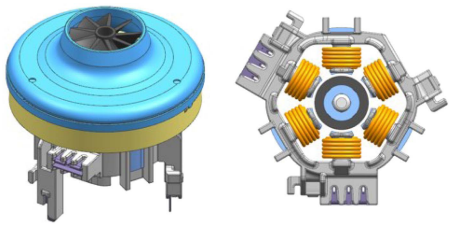

FIGURE 1. Original motor assembly with stator and rotor shapes.

TABLE 1. Specifications of Original Motor

List	Value
Pole/Slot	4 / 6
Wire/Winding type	Cu / Concentrated
Magnet type	ND bonded magnet
Operating speed range	30k–75 kr/min
Maximum input power	550 W

be utilized in various vacuum cleaners with different operating modes. Consequently, designing a motor with natural frequencies that avoid resonance across all operating modes becomes challenging. To address this issue, this article proposes an advanced method for altering the natural frequencies of motors. An additional structure with a variety of design factors was mounted on the stator of a motor to shift its natural frequencies. By modifying each design factor, the natural frequencies were shifted to target values, successfully avoiding any resonances. The results were validated through vibration and noise tests.

II. CHARACTERISTIC OF ORIGINAL MOTOR

A. SPECIFICATION OF ORIGINAL MOTOR

Fig. 1 and Table 1 show shape and specifications of a original vacuum cleaner motor. The stator of the motor is a concentrated winding configuration with six slots, and the rotor incorporates a bonded neodymium ring magnet with four poles. The motor's driving speed ranges from 30 000 to 75 000 r/min with a maximum input power is 550 W.

The fundamental frequency of the electromagnetic force in motors is determined by the number of rotor poles. In the four-pole motor, the frequency of the electromagnetic force is 4X, where 4X indicates four oscillations per rotor revolution. For conventional low-speed motors, electromagnetic force frequency resides at a lower range and does not pose significant issues, as low frequency noise is less perceptible to the human ears. However, in high-speed motors such as vacuum cleaner motors, the electromagnetic force frequency also increases, potentially contributing to motor noise. When resonance of the motor occurs, the noise level can increase significantly.

TABLE 2. Natural Frequency and Electromagnetic Force Frequencies of Original Motor Over Operating Mode

Electromagnetic force frequency (kHz)	Vacuum cleaner	Operating modes			
		Weak	Medium	Strong	Turbo
	A	2.8	3.5	4.5	-
	B	2.4	3.3	4.0	5.0
Natural frequency(kHz)		2.4			

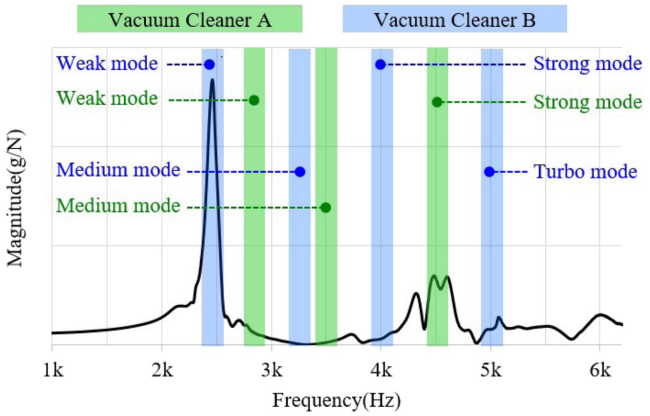

FIGURE 2. FRF of the original motor and frequency ranges of electromagnetic force.

B. NATURAL FREQUENCY ANALYSIS RESULT

The original motor is installed in two different cordless stick vacuum cleaners. Table 2 gives electromagnetic force frequencies and natural frequency of the motor for operating modes of two vacuum cleaners. Fig. 2 shows frequency response function (FRF) of the stator, which shows a distinct natural frequency at 2.4 kHz. Vacuum cleaner A has three operating modes based on suction power, while vacuum cleaner B has four operating modes.

In Fig. 2, bars represent the motor's electromagnetic force frequencies for each operating mode of the vacuum cleaners. Green bars correspond to electric force frequencies for vacuum cleaner A, and blue bars for vacuum cleaner B. The bar width indicates the range of the electromagnetic force frequency taking into account motor speed tolerance. The frequency range spans from −100 Hz to +100 Hz based on the central frequency, and the speed range extends from −1500 to +1500 r/min. In addition, natural frequency of the motors has a distribution due to tolerances of the motor and assembly tolerance.

Motor resonance can be avoided when the motor's natural frequency sufficiently deviates from the electromagnetic force frequencies. In Fig. 2, the natural frequency of the original motor avoids electromagnetic force frequencies for all the three operating modes of vacuum cleaner A, preventing motor resonance. However, in vacuum cleaner B, the natural frequency does not avoid the electromagnetic force frequency

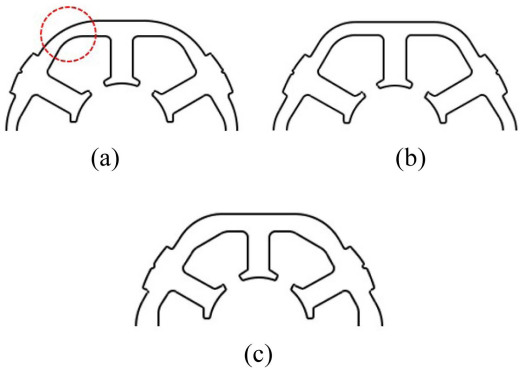

FIGURE 3. Stator core shapes. (a) Stator core of original motor. (b) Modified core 1. (c) Modified core 2.

in the weak mode, resulting in resonance. A peak at 4X frequency, the frequency of the electromagnetic force, is visible in Fig. 2. In order to prevent such motor resonance, it is essential to modify the motor's natural frequency.

III. RESONANCE AVOIDANCE THROUGH SHAPE MODIFICATION OF STATOR CORE

A. SPECIFICATION OF ORIGINAL MOTOR

To alter the motor's natural frequency, it is common to modify the stiffness of the motor's stator through changes in the stator core shape. The natural frequency f_n is represented as [2]

$$f_{\mathrm{n}} = \sqrt{\frac{K_{\mathrm{eq}}}{m}} \tag{1}$$

where K_{eq} is the equivalent stiffness of the stator and m is the mass of the stator. When the change in the mass of the stator is negligible, the motor's natural frequency is proportional to the stator's stiffness. The equivalent stiffness K_{eq} is expressed as

$$K_{\mathrm{eq}} = \frac{E_c h^3}{12 l^2} \tag{2}$$

where E_c is the elastic modulus, h is the stator yoke thickness, and l is the yoke's circumference. When the yoke's circumference l remains constant, the stator's stiffness K_{eq} is proportional to the yoke thickness h and thusly the natural frequency is also proportional to the yoke thickness h.

Fig. 3 displays the stator core shape of the original motor and shapes of modified cores. The stator core stiffness is altered by adjusting the yoke thickness, as indicated by the circle in Fig. 3(a). Fig. 3(a) represents the core shape of the original motor, Fig. 3(b) shows modified core 1, where the yoke thickness is reduced, and Fig. 3(c) illustrates modified core 2, where the yoke thickness is increased.

The target natural frequency for avoiding electromagnetic force frequencies for each operating mode of vacuum cleaner B should be less than 2.4 kHz, which is the electromagnetic force frequency for the weak mode, or positioned between the electromagnetic force frequencies for each operating mode in Fig. 2. Frequencies above 5.0 kHz in the turbo mode are excluded due to the significant increase in motor weight resulting from a substantial increase in stator core stiffness. As users hold cordless stick vacuum cleaner during operation, the limitation of motor weight must be considered when designing the motor.

TABLE 3. Modal Analysis and Iron Loss Analysis Results for Original Motor and Motors With Modified Cores

	Original motor	Motor with modified core 1	Motor with modified core 2
Natural frequency (kHz)	2.4	1.8	3.7
Iron loss (W)	15	18	14
Stator core weight (g)	51	47	57

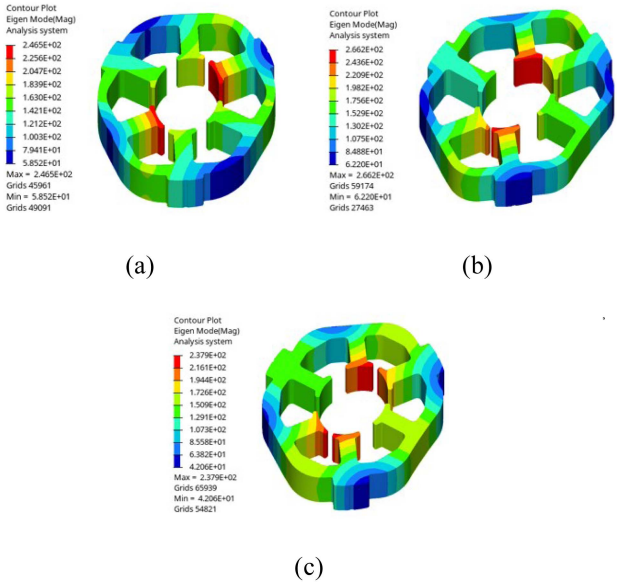

FIGURE 4. Modal analyses of stator cores. (a) Stator core of the original motor. (b) Modified core 1. (c) Modified core 2.

B. FEM MODAL ANALYSIS AND IRON LOSS ANALYSIS OF STATOR CORES

Table 3 gives the analysis results for natural frequency and iron loss associated with each stator core shape. The natural frequencies of the motors are calculated by finite element method (FEM) modal analysis of stator cores using ANSYS, and Fig. 4 shows the modal shape of each stator. The modal analysis result accounts for the effects of insulation and coil as well as stator core shape. Since the motor is set on a soft cushion such as sponge or rubber inside the vacuum cleaner, a free-free boundary condition was applied. The iron losses of motors are obtained by JMAG.

The natural frequency of the motor with the modified core 1 is 1.8 kHz, which meets the target frequency of less than 2.4 kHz. However, as the yoke thickness decreases, the magnetic flux density increases, leading to higher iron loss in the motor. If the motor with the modified core 1 has the same

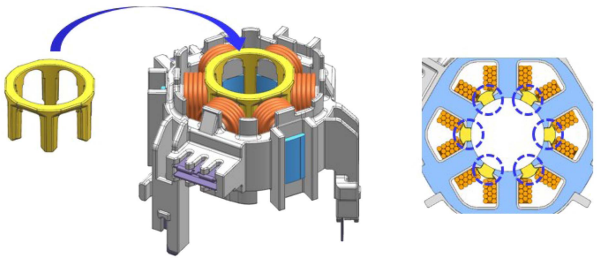

FIGURE 5. Installation of a cage-ring in the stator of the motor.

winding specifications as the original motor, its efficiency would decrease due to the increased iron loss.

The natural frequency of the motor with the modified core 2 is 3.7 kHz, which satisfies the target electromagnetic force frequency between 3.3 kHz for the medium mode and 4.0 kHz for the strong mode. The iron loss of the motor is reduced compared to the original motor, ensuring that the motor efficiency does not decrease. Therefore, in terms of stator core shape modifications to alter the natural frequency, the modified core 2 is preferable as it maintains motor efficiency.

C. COST AND MANUFACTURABILITY MODAL ANALYSIS AND IRON LOSS ANALYSIS OF STATOR CORES

Even minor modifications of the stator core shape necessitate additional molds for the stator core and insulations, leading to a significant increase in cost. Moreover, during motor production, productivity may decline due to the need to replace molds, parts and equipment in accordance with changes in production models. Furthermore, costs may rise whenever there is a need to modify the natural frequency to accommodate changes or additions to operating modes or to integrate new vacuum cleaners with different operating modes.

To address these concerns, a method was explored to enable the adjustment of the motor's natural frequency without changing the stator core shape.

IV. RESONANCE AVOIDANCE THROUGH SHAPE MODIFICATION OF STATOR CORE

A. ADDITIONAL COMPONENT: CAGE-RING

In order to change the motor's natural frequency, an additional component called a cage-ring is added to the motor, as shown in Fig. 5. When the cage-ring is fixed between the stator slots, the stator's stiffness increases, leading to a higher natural frequency for the motor.

B. CAGE-RING DESIGN FACTORS

As given in Table 4, the cage-ring design factors include the cage-ring material, contact length with the stator core, and the cage-ring shape. The motor's natural frequencies can vary depending on changes and combinations of these design factors. The optimal natural frequency, which allows the motor to avoid resonance, is determined from these variations. The configuration of the cage-ring was designed after the geometry of the stator core had been determined. The dimensions

TABLE 4. Cage-Ring Design Factors

No.	Design factor	Type 1	Type 2
1	Material (Tensile modulus)	PBT (11 500 MPa)	TPE (140 MPa)
2	Contact length with stator core	75% contact	100% contact
3	Shape	Shape 1	Shape 2

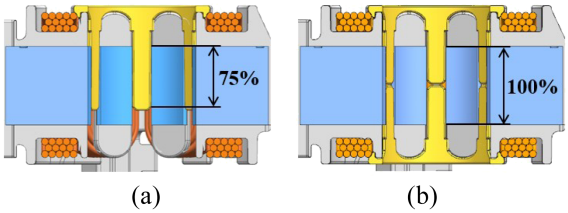

FIGURE 6. Contact length between a cage-ring and a stator core. (a) 75% contact; (b) 100% contact.

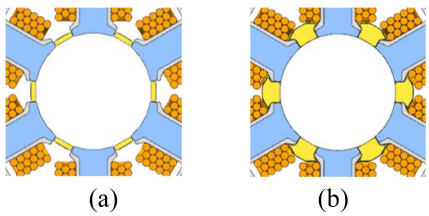

FIGURE 7. Cage-ring shapes. (a) Shape 1 and (b) shape 2.

and shape of the cage-ring were then modified to meet the dimensional constraints required for its integration into the stator.

The first design factor involves cage-ring materials: hard engineering plastic poly butylene terephthalate (PBT) and soft plastic thermo-plastic elastomer (TPE). The second design factor concerns contact lengths with stator core: 75% contact and 100% contact of the stator core height as demonstrated in Fig. 6. The third design factor pertains to the cage-ring shapes with two cases as shown in Fig. 7. Shape 1 of the cage-ring attaches only to the stator core, while shape 2 affixed to the stator core, insulation, and a portion of coil, thereby increasing the stator stiffness.

C. METHOD TO DETERMINE NATURAL FREQUENCY

There are two methods to check natural frequency of motors: One is to analyze natural frequency using three-dimensional (3-D) FEM, and the other is to measure natural frequency experimentally. In Table 3, 3-D FEM was used to evaluate the natural frequency based on the stator core shape. In this article, the natural frequency is measured by electron vibration force evaluation method. This technique measures the motor's natural frequency by utilizing the rotational torsion of the rotor.

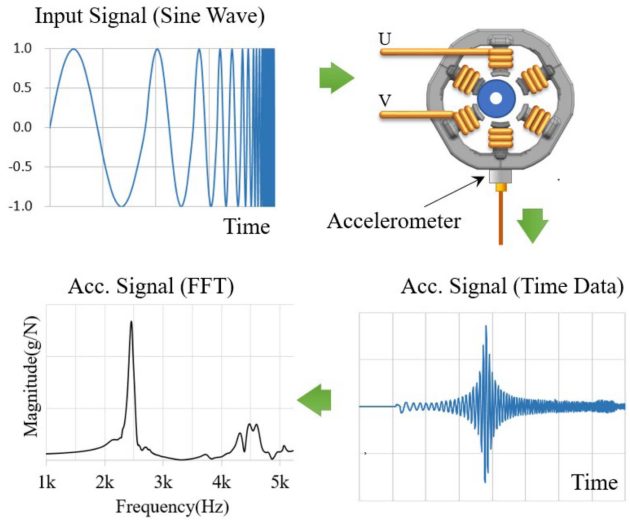

FIGURE 8. Electron vibration force evaluation.

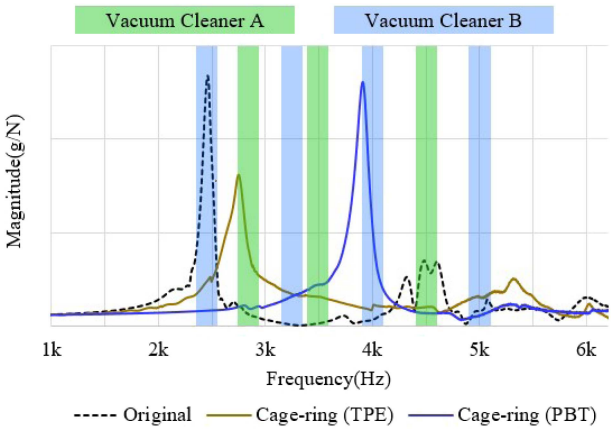

FIGURE 9. FRF analysis results with various cage-ring materials.

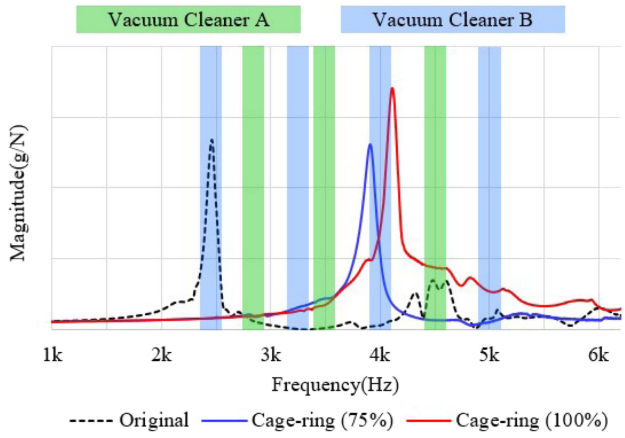

FIGURE 10. FRF analysis results with various contact length.

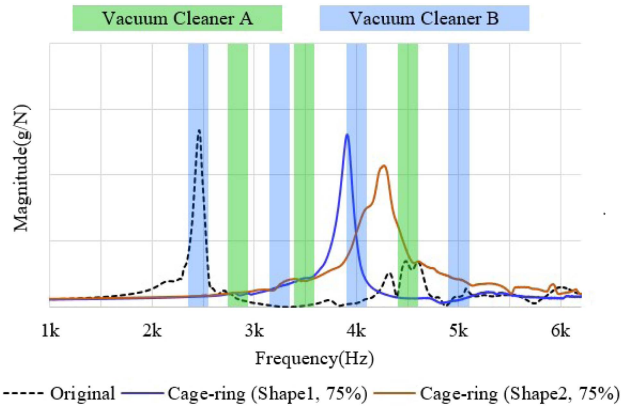

FIGURE 11. FRF analysis results with different cage-ring shapes at 75% contact length.

As shown in Fig. 8, the rotor contacts one side of the stator core. When an accelerated sine wave signal is applied to two-phase coils of the stator, the rotor, attached to the stator core, vibrates significantly at a specific frequency. At this point, the motor's natural frequency is measured by an accelerometer attached to the stator. Since the sine wave signal is applied to only two of three phases, the natural frequency can be measured without rotating the rotor.

D. NATURAL FREQUENCY MEASUREMENT RESULTS

Natural frequencies are compared based on the materials of the cage-ring. The contact length is 75% contact and the cage-ring shape is shape 1. When the cage-ring material is hard plastic PBT, the natural frequency increases from 2.4 to 3.9 kHz as shown in Fig. 9. The natural frequency does not avoid the electromagnetic force frequency of the motor in the medium mode of vacuum cleaner B, which is likely to cause resonance in the motor. When the cage-ring material is soft plastic TPE, the natural frequency increases to 2.8 kHz as presented in Fig. 9. Because the natural frequency is outside the range of the electromagnetic force frequencies in all operating modes of vacuum cleaner B, the motor resonance does not occur. In addition, it is observed that the natural frequency change depends on the rigidity of the cage-ring material. The higher the rigidity of the cage-ring material, the higher the natural frequency of the motor.

Natural frequencies are compared based on the contact lengths between the cage-ring and stator core. Material of the cage-ring is PBT and the shape of the cage-ring is shape 1. As the contact length changes from 75% contact to 100% contact, the natural frequency rises from 3.9 to 4.1 kHz as shown in Fig. 10. As the contact length increases, the stiffness of the stator increases and natural frequency of the motor also increases. However, in both cases, the natural frequencies of the motor do not avoid the electromagnetic force frequency in the medium mode of vacuum cleaner B, which is likely to cause resonance in the motor.

Natural frequencies are compared based on the shapes of the cage-ring. The material of the cage-ring is PBT, and the contact length is 75% contact. As the cage-ring shape changes from shape 1 to shape 2, the natural frequency increases from 3.9 to 4.3 kHz as shown in Fig. 11. When the cage-ring shape

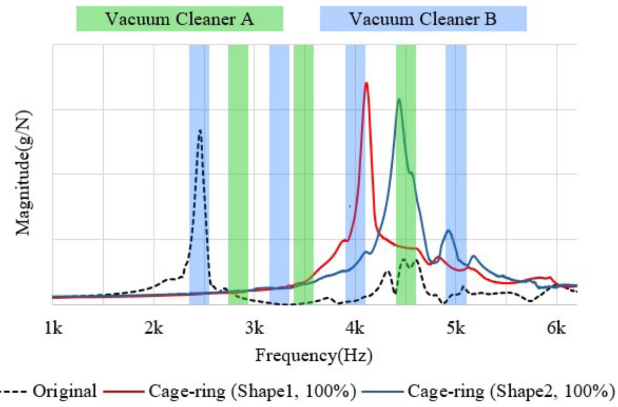

FIGURE 12. FRF analysis results with different cage-ring shapes at 100% contact length.

TABLE 5. Natural Frequencies of the Motor Based on the Design Factors of the Cage-Ring

No.	Material	Contact length	Shape	Natural frequency (kHz)	Predict resonance
1	TPE	75%	Shape 1	2.8	×
2	PBT	75%	Shape 1	3.9	○
3	PBT	100%	Shape 1	4.1	○
4	PBT	75%	Shape 2	4.3	○
5	PBT	100%	Shape 2	4.5	×
6	Original motor			2.4	○

is shape 2, the natural frequency of motor manages to avoid the electromagnetic force frequencies in all modes of vacuum cleaner B, preventing motor resonance.

In addition, after changing the contact length between the cage-ring and the stator core from 75% contact to 100% contact, the natural frequencies of the motor are measured. As shown in Fig. 12, when the contact length is 100% contact, the natural frequency of the motor rises from 4.1 to 4.5 kHz as the shape of the cage-ring changes from shape 1 to shape 2. The natural frequency of the motor manages to avoid the frequencies of the electromagnetic force frequencies in all operating modes of vacuum cleaner B, ensuring that resonance of the motor does not occur.

Table 5 gives the measured results of the motor's natural frequencies according to changes and combinations of the three design factors. The natural frequency of the motor varied from 2.8 to 4.5 kHz, and the natural frequency that avoids resonance was found in all operating modes of vacuum cleaner B. Moreover, using this approach, it is possible to identify a natural frequency capable of avoiding motor resonance in other vacuum cleaners having different driving modes and therefore different electromagnetic forces.

E. EXPERIMENTAL VALIDATION

The design method is verified through a noise test of the motor. In the weak mode of vacuum cleaner B, the noises of

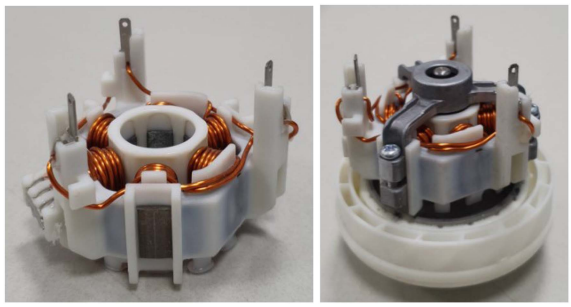

FIGURE 13. Stator and motor assembly with the cage-ring.

FIGURE 14. Noise and vibration measurement apparatus.

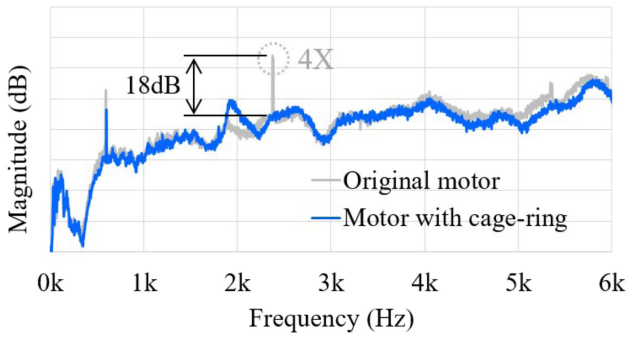

FIGURE 15. Noise measurement result of the original motor and the motor with the cage-ring.

the motor with the cage-ring and the original motor without the cage-ring are compared. The motor designated as no. 5 in Table 5 used for the motor with the cage-ring. Its natural frequency is 4.5 kHz, which avoids the electromagnetic force frequencies in all operating modes of vacuum cleaner B. The cage-ring material is PBT, contact length is 100% contact, and the cage-ring shape is shape 2.

Fig. 13 shows the stator and motor with the cage-ring reflecting the design factors, and Fig. 14 illustrates the noise testbed of the motor. Fig. 15 presents the noise test result of the motors, showing the FFT spectrum of noise generated by the vacuum cleaner motor. The blue line represents the noise level of the motor with the cage-ring, and the gray line is noise level of the original motor. In the original motor, the 4X peak component of 2.4 kHz is clearly discernible, and it can contribute to an increase in overall motor noise and generate an unpleasant, abnormal noise perceptible to the human ears. However, the 4X peak component is not present in the motor with the cage-ring. The 4x peak component of the motor

noise with the cage-ring was reduced by avoiding resonance. The reduced 4x peak noise was concealed in the base noise because the vacuum cleaner motor had a very large base noise due to the air flow.

V. CONCLUSION

A method has been developed to alter the natural frequencies of motors without modifying the stator core shape. By incorporating a cage-ring and adjusting its design factors in various combinations, the natural frequencies of motors can be significantly changed. This approach effectively avoids motor resonances associated with various electromagnetic force frequencies, such as those found in vacuum cleaner motors. In particular, it is advantageous to employ one motor across various vacuum cleaners with different operating modes.

As the stator core shape remains unchanged, there is no need for additional production of stator core, insulating molds and/or assembly equipment. This provides substantial benefits in terms of cost, productivity, and manufacturing management for motors. Eliminating the need for additional molds for the stator core and insulation can result in savings over one hundred thousand dollars.

In addition, combining the stator core and cage-ring designs, and improving the numerical analysis accuracy of the cage-ring from the start of the motor design would be highly beneficial for design and evaluation.

REFERENCES

[1] D.-Y. Kim, M.-R. Park, J.-H. Sim, and J.-P. Hong, "Advanced method of selecting number of poles and slots for low-frequency vibration reduction of traction motor for elevator," *IEEE/ASME Trans. Mechatronics*, vol. 22, no. 4, pp. 1554–1562, Aug. 2017.

[2] G.-D. Lee, M.-C. Kang, and G.-T. Kim, "The equilibrium design of radial magnetic force for reduction of vibration in IPM type BLDC," in *Proc. IEEE Int. Elect. Mach. Drives Conf.*, 2015, pp. 555–561.

[3] G. Lee, G. Kim, H. Shin, and C. Kim, "The optimum design of interior permanent magnet synchronous motor for the vibration reduction," in *Proc. Int. Conf. Elect. Mach. Syst.*, 2015, pp. 227–231.

[4] Q. Wang, K. Yan, H. Li, and M. Yuan, "Motor noise source identification based on frequency domain analysis," in *Proc. Int. Conf. Mechatronics Automat.*, 2009, pp. 2373–2377.

[5] S. Park, W. Kim, and S.-I. Kim, "A numerical prediction model for vibration and noise of axial flux motors," *IEEE Trans. Ind. Electron.*, vol. 61, no. 10, pp. 5757–5762, Oct. 2014.

[6] I.-S. Jang et al., "Method for analyzing vibrations due to electromagnetic force in electric motors," *IEEE Trans. Magn.*, vol. 50, no. 2, pp. 297–300, Feb. 2014.

[7] K. N. Srinivas and R. Arumugam, "Static and dynamic vibration analyses of switched reluctance motors including bearings, housing, rotor dynamics, and applied loads," *IEEE Trans. Magn.*, vol. 40, no. 4, pp. 1911–1919, Jul. 2004.

[8] W. Sanchez, C. Carvajal, J. Poalacin, and E. Salazar, "Detection of cavitation in centrifugal pump for vibration analysis," in *Proc. 4th Int. Conf. Control, Automat. Robot.*, 2018, pp. 460–464.

[9] S. Li, X. Zhang, and Z. Wei, "The study and optimization of noise in a fuel pump," in *Proc. CSAA/IET Int. Conf. Aircr. Utility Syst.*, 2018, pp. 466–470.

[10] Y. Choo et al., "Investigation of systematic efficiency in a high-speed single-phase brushless DC motor using multi-physics analysis for a vacuum cleaner," *IEEE Trans. Magn.*, vol. 55, no. 7, Jul. 2019, Art. no. 8203606.

[11] K. B. Jang, S. H. Won, T. H. Kim, and J. Lee, "Starting and high-speed driving of single-phase flux-reversal motor for vacuum cleaner," *IEEE Trans. Magn.*, vol. 41, no. 10, pp. 3967–3969, Oct. 2005.

[12] J.-Y. Lim, Y.-C. Jung, S.-Y. Kim, and J.-C. Kim, "Single phase switched reluctance motor for vacuum cleaner," in *Proc. IEEE Int. Symp. Ind. Electron.*, 2001, vol. 2, pp. 1393–1400.

[13] Z. Han, J. Liu, C. Gong, and J. Lu, "Influence mechanism on vibration and noise of PMSM for different structures of skewed stator," in *Proc. 20th Int. Conf. Elect. Mach. Syst.*, 2017, pp. 1–5.

[14] M.-R. Park, J.-W. Jung, D.-Y. Kim, J.-P. Hong, and M.-S. Lim, "Design of high torque density multi-core concentrated flux-type synchronous motors considering vibration characteristics," *IEEE Trans. Ind. Appl.*, vol. 55, no. 2, pp. 1351–1359, Mar./Apr. 2019.

[15] S. Wang, J. Hong, Y. Sun, and H. Cao, "Exciting force and vibration analysis of stator permanent magnet synchronous motors," *IEEE Trans. Magn.*, vol. 54, no. 11, Nov. 2018, Art. no. 8108205.

[16] J.-W. Jung, S.-H. Lee, G.-H. Lee, J.-P. Hong, D.-H. Lee, and K.-N. Kim, "Reduction design of vibration and noise in IPMSM type integrated starter and generator for HEV," *IEEE Trans. Magn.*, vol. 46, no. 6, pp. 2454–2457, Jun. 2010.

[17] F. Ishibashi, M. Matsushita, S. Noda, and K. Tonoki, "Change of mechanaical natural frequencies of induction motor," *IEEE Trans. Ind. Appl.*, vol. 46, no. 3, pp. 922–927, May/Jun. 2010.

[18] H. Yin, F. Ma, X. Zhang, C. Gu, H. Gao, and Y. Wang, "Research on equivalent material properties and modal analysis method of stator system of permanent magnet motor with concentrated winding," *IEEE Access*, vol. 7, pp. 64592–64602, 2019.

[19] S.-H. Lee, J.-P. Hong, S.-M. Hwang, W.-T. Lee, J.-Y. Lee, and Y.-K. Kim, "Optimal design for noise reduction in interior permanent-magnet motor," *IEEE Trans. Ind. Appl.*, vol. 45, no. 6, pp. 1954–1960, Nov./Dec. 2009.

[20] J. Shou, J. Ma, B. Xu, L. Qiu, C. Luo, and Y. Fang, "Noise optimization of high-speed permanent magnet motor by stiffeners," in *Proc. IEEE Transp. Electrific. Conf. Expo, Asia-Pac.*, 2022, pp. 1–6.

WOONG HWANG received the M.S. degrees in mechanical engineering from Ajou University, Suwon-si, South Korea, in 2000.

He is currently a Senior Engineer with the Energy Technology Laboratory, Digital Appliances, Samsung Electronics, Suwon-si, South Korea. His primary responsibilities include design and optimization of electric machine. Throughout his industrial career, he has developed various electric machines for home appliances.

JIMIN KIM received the B.S. and Ph.D. degrees in mechanical engineering and automotive engineering from Hanyang University, Seoul, South Korea, in 2009 and 2017, respectively.

He is currently a Staff Engineer with the Energy Technology Lab, Digital Appliances, Samsung Electronics, Suwon-si, South Korea. His primary responsibilities include design and optimization of electric machine and analysis of noise and vibration. Throughout his industrial career, he has developed various electric machines for cordless vacuum cleaners.

JIHOON HAN received the B.S. and M.S. degrees in aerospace engineering from Korea Advanced Institute of Science and Technology (KAIST), Daejeon, South Korea, in 1997 and 1999, respectively.

He is currently a Principle Engineer, Digital Appliances, Samsung Electronics, Suwon-si, South Korea. His primary responsibilities include analyzing Noise and vibration of motors and improve the structural performance of motors and compressors. Throughout his academic and industrial career, he has developed various motors models such as balancing method for mass production of small and high speed fan motor for vacuum cleaners and analysis of noise and vibration in electric motors and compressors for home appliances.

WONSOO KANG received the B.S. degrees in mechanical engineering from Sungkyunkwan University, Seoul, South Korea, in 2009.

He is currently is a Staff Engineer with the Energy Technology Laboratory, Digital Appliances, Samsung Electronics. His primary responsibilities include designing the mechanical structure of motors. Throughout his industrial career, he has developed various mechanical parts in electric motors and refrigerator for home appliances.

SUNGHYUK PARK received the B.S. and M.S. degrees in mechanical design and production engineering from Seoul National University, Seoul, South Korea, in 1998 and 2000, respectively, and the Ph.D. degree in mechanical engineering from the University of Illinois at Urbana-Champaign, Champaign, IL, USA, in 2007.

He is currently a Senior Engineer with the Energy Technology Laboratory, Digital Appliances, Samsung Electronics, Suwon-si, South Korea. His primary responsibilities include analyzing the structural robustness and performance of motors and compressors. Throughout his academic and industrial career, he has developed various numerical models such as cutting force prediction models and analysis of noise and vibration in electric motors and compressors for home appliances.